Available online at www.sciencedirect.com
SCIENCE DIRECT®
Journal of Molecular Catalysis A: Chemical 221 (2004) 81–88
JOURNAL OF MOLECULAR CATALYSIS A: CHEMICAL
www.elsevier.com/locate/molcata

Preparation of activated carbon fibers supported TiO_2 photocatalyst and evaluation of its photocatalytic reactivity

Pingfeng Fu, Yong Luan, Xuegang Dai*

Institute of Process Engineering, Chinese Academy of Sciences, Beijing 100080, PR China

Received 12 February 2004; received in revised form 7 June 2004; accepted 11 June 2004
Available online 30 July 2004

Abstract

Activated carbon fibers (ACFs) supported TiO_2 photocatalyst was successfully prepared by a molecular adsorption–deposition (MAD) method followed by calcination in a stream of Ar gas. The photocatalyst developed was characterized by SEM, XRD, XPS, BET surface area and UV–vis adsorption spectroscopy. SEM observation showed TiO_2 was deposited on almost each carbon fiber with a coating thickness of about 100 nm, and the space between adjacent fibers was remained unfilled to allow UV light to penetrate into the felt-form photocatalyst to a certain depth. Anatase-form TiO_2 was uniquely developed even as calcination temperatures rose up to 900 °C. Tight contact of thin TiO_2 coating to carbon fibers surfaces was supposed to suppress phase transformation of TiO_2 from anatase to rutile, and to keep high crystallinity of anatase. As confirmed by XRD and XPS examinations, the micrographic structure and surface properties of ACFs had not been damaged by the deposition process and calcination at high temperatures.

The present photocatalyst showed high photocatalytic reactivity in photodegradation of highly concentrated methylene blue (MB) solutions. The comparative experiments indicated the photocatalyst produced had a combined effect of photocatalytic reactivity of anatase-type TiO_2 with adsorptive property of activated carbon fibers. In addition, the possibility of cyclic usage of the photocatalyst was also confirmed.

Keywords: Molecular adsorption–deposition method; Activated carbon fibers; Titanium dioxide; Photocatalytic reactivity; Degradation

1. Introduction

Anatase-type TiO_2 has attracted much attention for its potential application in decomposition of various environmental pollutants in both gaseous and liquid phases [1]. The photocatalytic degradation systems using fine TiO_2 powder under UV irradiation have been widely investigated [2–4]. However, separation of the fine TiO_2 powder from the solution after degradation is time consuming and costly [5]. Development of TiO_2 photocatalysts anchored on supporting materials with large surface areas, by which dilute polluted substances could be condensed, would be of great significance, not only to avoid the disadvantages of filtration and suspension of fine photocatalyst particles, but to lead to high photodecomposition efficiency [6]. Recently, supported TiO_2 photocatalysts on various porous materials were prepared by a pasting treatment [7], a sol–gel method [8], or an ionized cluster beam (ICB) method [6].

Granular activated carbons (GACs), widely used as an effective adsorbent in treating polluted water and gas, has been introduced as a support for TiO_2 photocatalyst in some studies, and photocatalytic reactivity and principles of enhancing photodecomposition process by activated carbon have also been addressed in detail [9–12]. Activated carbon fibers (ACFs) are one kind of highly microporous carbon materials, having a larger pore volume and a more uniform micropore size distribution than granular activated carbons [13–15]. Generally, activated carbon fibers are considered to have larger adsorption capacity and greater rates of adsorption and desorption process than granular activated carbons. However, so far there have been only a few reports to study preparation methods and applications of activated carbon fibers supported TiO_2 photocatalysts. Reported methods of depositing

* Corresponding author. Tel.: +86 10 62533616; fax: +86 10 62561822.
E-mail address: xgdai@home.ipe.ac.cn (X. Dai).

1381-1169/$ – see front matter © 2004 Elsevier B.V. All rights reserved.
doi:10.1016/j.molcata.2004.06.018

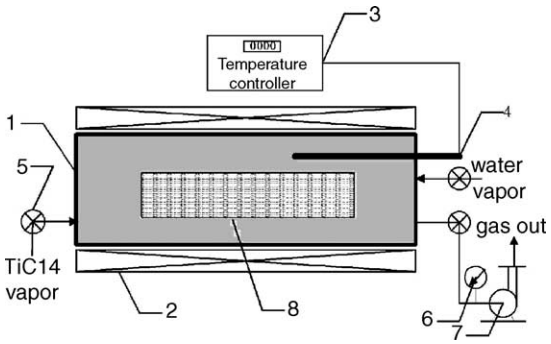

Fig. 1. Schematic diagram of MAD apparatus. (1) Quartz glass tube, (2) heating device, (3) temperature controller, (4) thermal sensor, (5) vacuum valve, (6) vacuometer, (7) vacuum pump, (8) activated carbon fibers.

TiO_2 photocatalysts on ACFs include an ionized cluster beam [6], an impregnation method [16], and a coating treatment by loading commercial TiO_2 powder on ACFs with polymer binders [17]. Precipitation of titania coating on microporous carbon surface by a molecular adsorption–deposition (MAD) method was once studied by Matsumoto et al. [18] to modify carbon surface to improve its adsorptive properties for gases. In this paper, this method will be introduced as a new way to prepare ACFs supported TiO_2 photocatalyst with the expectation of combining the effects of high adsorption capacity of ACFs and photocatalytic reactivity of anatase-type TiO_2.

In the present study, the preparation of activated carbon fibers supported TiO_2 photocatalyst and its characterization are addressed in detail. The effective photocatalytic reactivity of the photocatalyst produced has been demonstrated by its photocatalytic degradation of highly concentrated mythylene bule (MB) solutions. The stability of the photocatalyst prepared in the stirred solutions has also been discussed.

2. Experimental

2.1. Titanium dioxide coating by molecular adsorption–deposition method

Viscose rayon-based activated carbon fibers in felt form (Zichuan Carbon Fibers Co. Ltd. in Hebei Province, China), having a specific surface area of 933.8 $m^2\,g^{-1}$, were used in this study. The reaction chamber was a quartz glass tube sealed at both ends by vacuum valves, and the schematic diagram of MAD apparatus is shown in Fig. 1.

A piece of ACFs felt was first treated in boiling water for 30–50 min, then dried and put into the reaction chamber which was evacuated at 403 K and 10^{-2} Torr for 2 h prior to adsorption of a controlled amount of pure $TiCl_4$ vapor at 293 K. For a certain period, the adsorbed $TiCl_4$ film was reacted with saturated water vapor at 298 K to yield a hydroxylate titania coating. The system was then evacuated at 363 K and 10^{-2} Torr for 30 min after the $TiCl_4$ hydrolysis, and the hydroxylate titania-coated ACFs were calcined at ambient pressure in Ar gas at different temperatures for 1.5 h to form TiO_2 coating. By adjusting the vapor pressure of $TiCl_4$ and adsorption time, thickness of TiO_2 coating could be controlled. The activated carbon fibers supported TiO_2 photocatalyst will be expressed as TiO_2/ACFs-*n*, where *n* is the amount of coated titanium dioxide in milligrams per unit weight of ACFs. The value *n* was determined from an ignition loss of the photocatalyst TiO_2/ACFs-*n* calcined at 700 °C for 5 h in a stream of air.

2.2. Instrumental analysis of ACFs supported TiO_2 photocatalyst

Scanning electron micrographs (SEM) of the photocatalyst were performed using a SEM apparatus (Cambridge S250 MK2, operated at 20 kV). X-ray diffraction patterns of original ACFs, hydroxylate titania-coated ACFs, and ACFs supported TiO_2 photocatalysts calcined at different temperatures were obtained by using an automatic X-ray diffractometer with Cu Kα radiation (Rigaku D/max 2200PC, operated at 40 kV and 40 mA). Specific surface area analysis of the photocatalysts was carried out by Brunau–Emmet Teller (BET) method using an Autosorb-1 (ASIMP Quantchrome, USA) with nitrogen adsorption at 77 K. The measured samples were evacuated at 473 K and 10^{-5} Torr for 13 h prior to the adsorption measurements. UV–vis adsorption spectroscopy measurements were performed by using a UV–visible diffuse reflectance spectrophotometer (Shimadzu UV-2100) at 298 K, with the aims of assessing the presence of quantum size effects, location of adsorption edges of the photocatalysts and UV adsorption intensity.

XPS analysis of the photocatalyst calcined at 800° for 1.5 h was carried out using an ESCALAB MarkII Spectrophotometer equipped with two ultrahigh-vacuum chambers in which the pressure during the measurements was about 10^{-7} Torr. An Al Kα X-ray source ($h\gamma$ = 1486.6 eV)was used for the excitation of electrons. The analyzer was operated at 50 eV pass energy for high solution spectra. The carbon C1s electron binding energy (B.E.) corresponding to graphitic carbon was referenced at 284.60 eV for calibration purpose.

Table 1
Specific surface areas (S_{BET}) of unmodified ACFs and the TiO_2/ACFs photocatalysts

Samples	Unmodified ACFs	TiO_2/ACFs-191	TiO_2/ACFs-327	TiO_2/ACFs-418
TiO_2 loading (mg g^{-1})	–	191	327	418
S_{BET} ($m^2\,g^{-1}$)	933.8	592.9	419.5	321.4

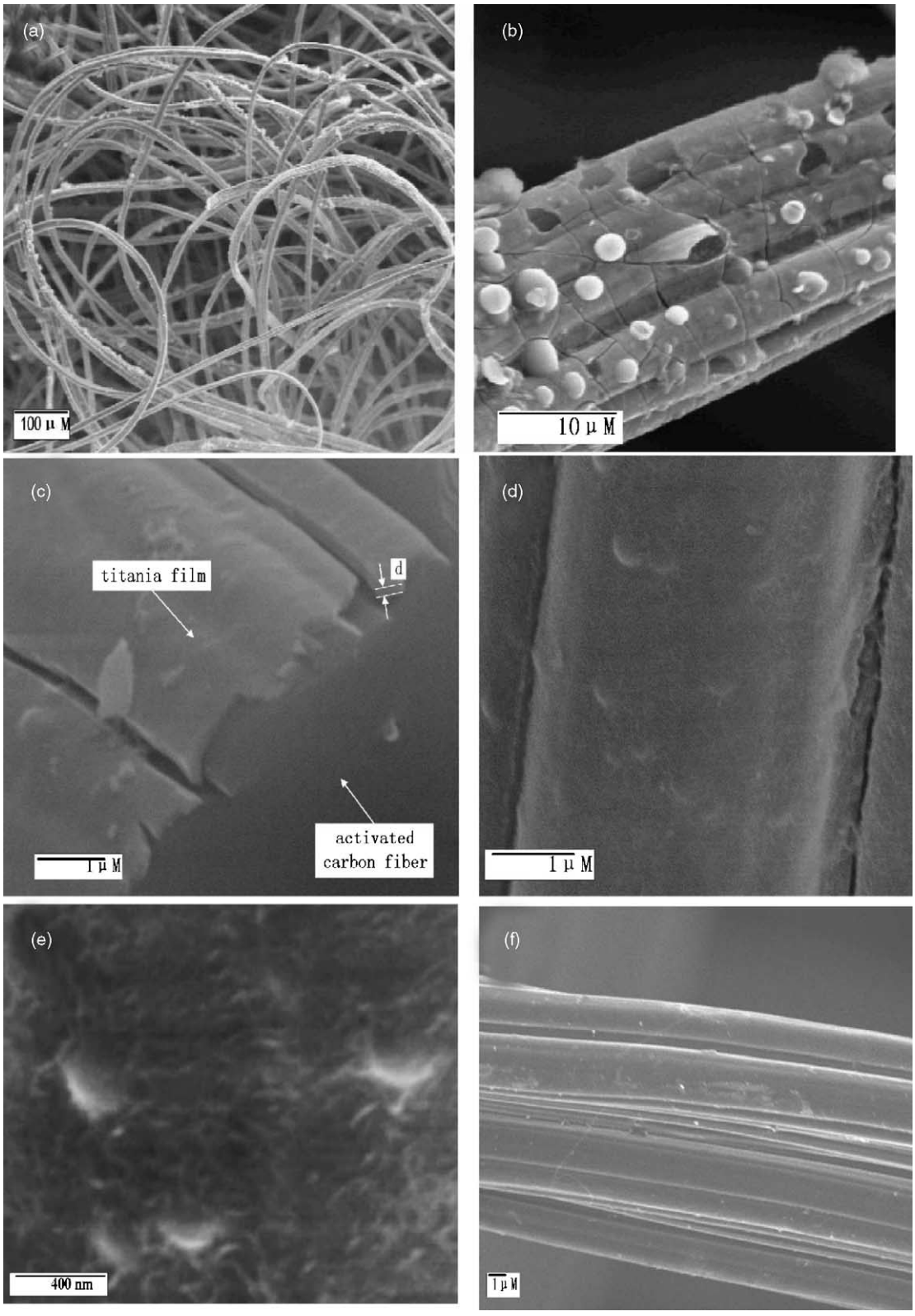

Fig. 2. SEM micrographs of the TiO_2/ACFs photocatalyst and unmodified ACFs, (a) general view of the photocatalyst, 100×; (b) TiO_2 coating on single carbon fiber, 2000×; (c) cross-sectional view of TiO_2 coating, 20,000×; (d) surface of TiO_2 coating, 20,000×; (e) surface of TiO_2 coating, 50,000×;and (f) single unmodified activated carbon fiber 4000×.

2.3. Photocatalytic degradation of methylene blue (MB)

The aqueous solution of methylene blue with an initial concentration of 2.498 mmol/L for experiments was prepared from distilled water and reagent-grade MB. Two pieces of the prepared TiO_2/ACFs in felt form, with a size of 90 mm length, 55 mm width and 2 mm thickness, were symmetrically placed on two sides of a Ø 80 mm × 95 mm Pyrex reaction cell, and exposed to a 24 W low pressure mercury lamp (dominant wavelength: 254 nm) fixed along the axis of the reaction cell. The distance between lamp tube and photocatalyst surface is about 12 mm. For each experiment operation, 400 mL of MB solution with the same initial concentration was transferred into the reaction cell and stirred by blowing air at a flow rate of 90 mL min^{-1} which could also provide dissolved oxygen for photocatalytic reaction. When the MB solution was put into the reaction cell, UV light was turned on to carry out experiments of photolysis, photolysis and adsorption of unmodified ACFs, and photocatalytic degradation by the TiO_2/ACFs photocatalysts. The photodecomposition reaction process was monitored by sampling 2 mL processed solutions at appropriate intervals for measurement of absorbance using a UV–vis 9100 spectrophotometer.

3. Results and discussion

3.1. Characterization of ACFs supported TiO_2 photocatalyst

3.1.1. Specific surface areas and deposited TiO_2 amount of the photocatalysts

Three measured TiO_2/ACFs photocatalysts listed in Table 1 have been calcined at 700 °C for 1.5 h. As shown in Table 1, the specific surface areas (S_{BET}) of the photocatalysts decrease with the increase of TiO_2 contents, indicating that TiO_2 coverage of carbon fibers becomes higher while the amount of the adsorbed $TiCl_4$ vapor increases. The increased TiO_2 coverage results in greatly reducing original surface areas and micropore volume of carbon fibers. However, the photocatalyst TiO_2/ACFs-418 with a maximum content of TiO_2 still has the S_{BET} of 321.4 m^2 g^{-1}. Therefore, the TiO_2 coverage in this sample is not so high yet because the S_{BET} value is determined by the unit weight of ACFs and coated TiO_2, indicating that certain amount of carbon fibers is still exposed in this photocatalyst. For the photocatalytic degradation of dilute pollutants, exposed carbon fiber surfaces will service as centers of condensing substrates with a physical adsorption process, and the condensed substrates would be transferred to neighboring TiO_2 particles by surface diffusion after the substrates around TiO_2 have been degraded [11,19].

3.1.2. SEM and XRD analysis

TiO_2/ACFs photocatalyst prepared by the molecular adsorption–deposition method is in the form of 2 mm thick felt. SEM micrographs in Fig. 2 shows morphologies of the photocatalyst calcined at 700 °C and the unmodified ACFs.

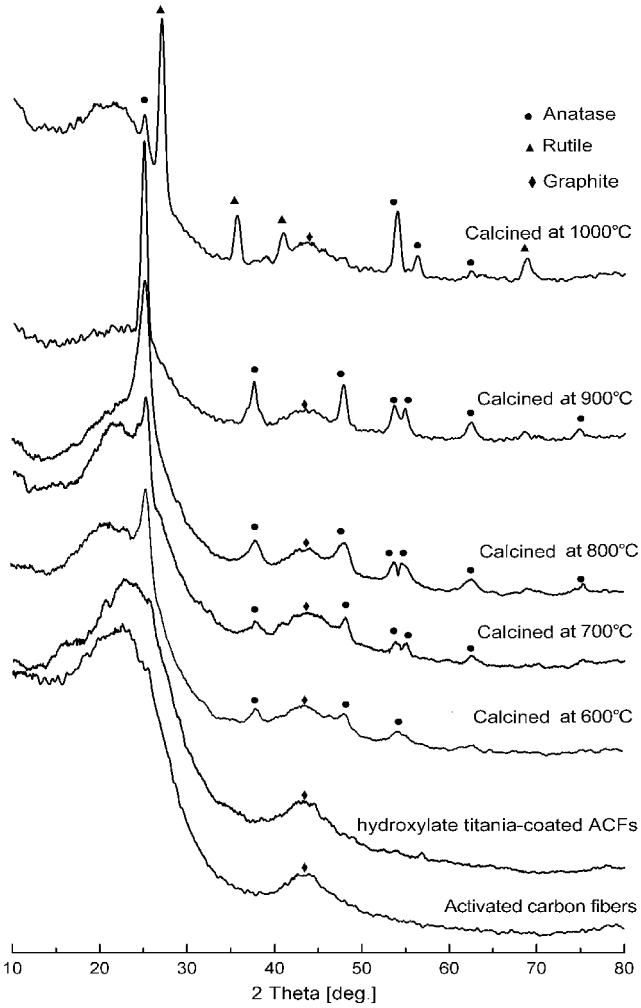

Fig. 3. XRD patterns of unmodified ACFs, hydroxylate titania-coated ACFs, and ACFs supported TiO_2 photocatalysts calcined at different temperatures.

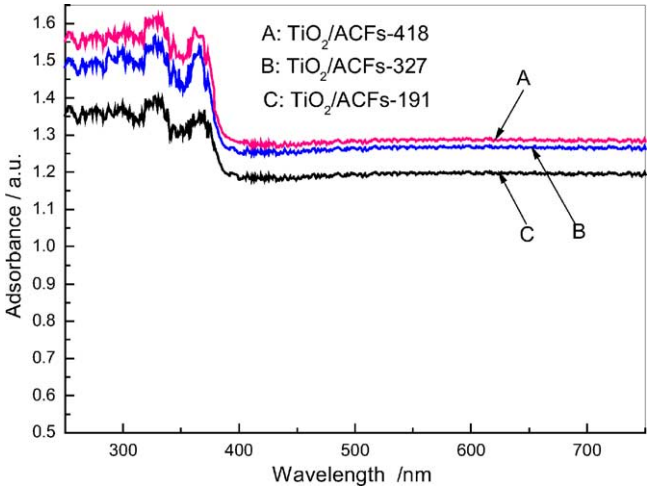

Fig. 4. UV–vis diffuse reflectance spectra of ACFs supported TiO_2 photocatalysts.

Fig. 2a shows TiO_2 coating has been immobilized onto almost each fiber of ACFs. Although TiO_2 coating has been deposited on fibers at such a large scale, the TiO_2/ACFs still retains the same spatial distribution of carbon fibers as in their unmodified state. Therefore, adequate UV irradiation can penetrate into the felt-form photocatalyst to a certain depth to form a three dimensional environment for photocatalytic reaction. This feature differentiates the present photocatalyst from such current immobilizing photocatalysts as immobilized TiO_2 on the surfaces of glass substances [9], silica gel [20], steel plate [21] and ceramic membranes [22], which could only provide two dimensional surface for photodegradation. As shown in Fig. 2b and c, TiO_2 coating could be considered as a layer in spite of small deposited TiO_2 particles on the layer. Due to shrinkage of the hydroxylate titania coating during calcination treatment and long grooves on carbon fiber surface shown in Fig. 2f, the resulting TiO_2 layer on carbon fibers shown in Fig. 2b and c is split into numerous flakes. The thickness of TiO_2 layer can be estimated to be about 100 nm from Fig. 2c. Fig. 2d and e show the surface morphology of TiO_2 coating with larger magnitudes. The surface of TiO_2 layer is not so homogenous, and especially rib and furrow structure is clearly shown on the layer surface. The rough surface of TiO_2 layer may contribute to increasing the surface area of loaded TiO_2, which could offer greater chance to adsorb substrates onto TiO_2 surface. The surface morphology of the present TiO_2 layer is different from that of the coating developed by an ionized cluster beam method, where the TiO_2 was deposited on the ACFs as small clusters [6].

In Fig. 3, X-ray diffraction patterns of unmodified ACFs, hydroxylate titania-coated ACFs, and ACFs supported TiO_2 photocatalysts calcined at different temperatures are compared. The broad diffraction peak at 43.6° of the unmodified ACFs is attributed to the reflections from both (1 0 0) and (1 0 1) planes of graphite [18,33]. While the calcination tem-

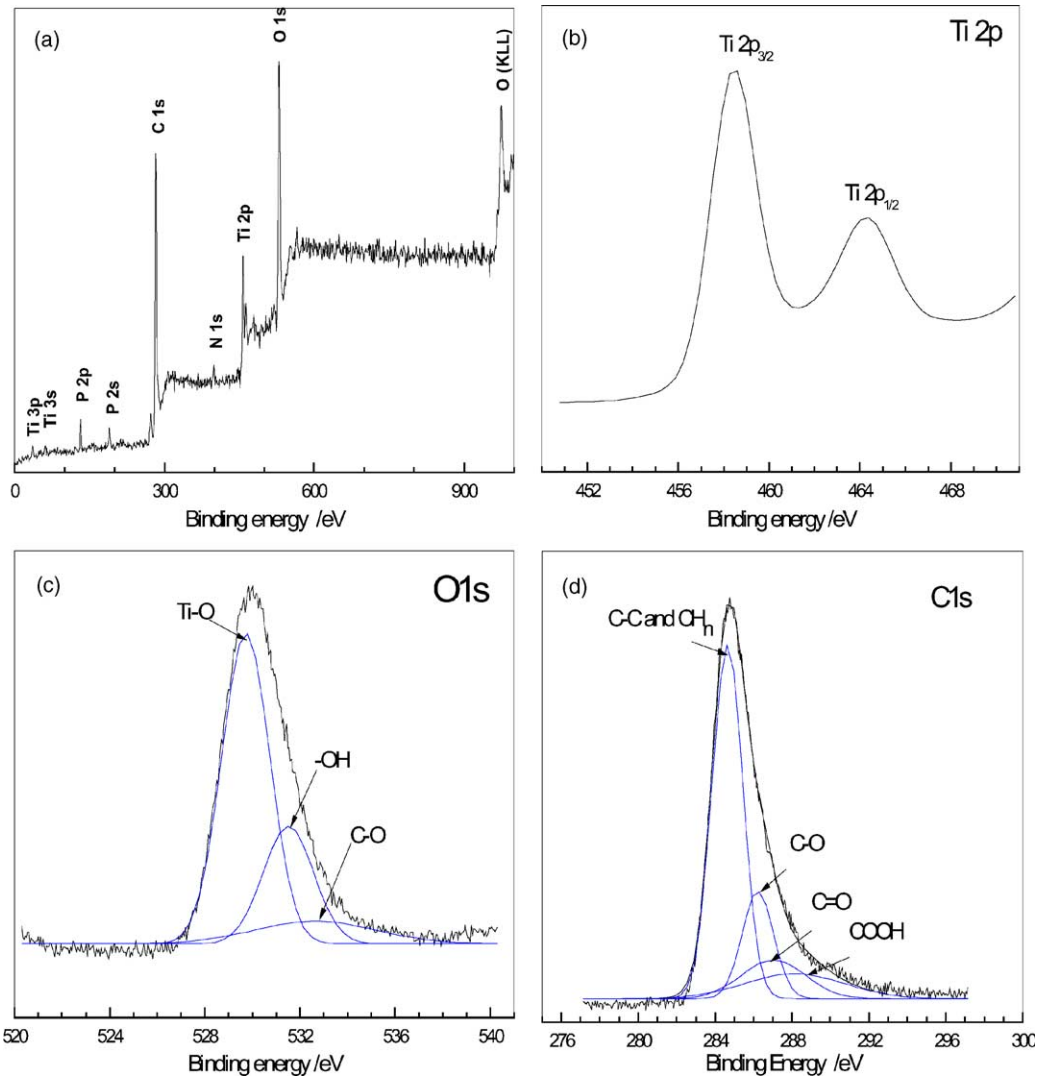

Fig. 5. (a) XPS survey spectrum for the surface of ACFs supported TiO_2 photocatalyst, (b–d) XPS spectra of individual lines of Ti2p, O1s and C1s measured at high resolution, respectively.

peratures rise up to1000 °C, this typical peak still appears in the XRD patterns of the photocatalysts prepared. This characteristic indicates micrographic structure of ACFs has not been damaged with TiO_2 deposition and calcination at high temperatures.

XRD patterns of ACFs supported TiO_2 photocatalysts show that all of the photocatalysts have developed unique anatase-type TiO_2 when the calcination temperatures are lower than 1000 °C. As the calcination temperature increases, the photocatalysts show sharper diffraction peaks, which indicates the improvement in crystallinity of anatase-type structure. However, when heat treatment temperature even increases to 900 °C, separation of 1 0 3, 0 0 4 and 1 1 2 diffraction peaks of anatase-form is not clearly detected yet. Therefore, the improvement in crystallinity of anatase is not so pronounced for the present photocatalysts. At the same time, the anatase-type structure is still kept even after the photocatalyst is calcined at 1000 °C for 1.5 h. The phenomena mentioned above can be attributed to two following facts that thin TiO_2 layers are tightly contacted to the carbon fibers surfaces, and carbon surfaces located under TiO_2 layers can suppress phase transformation of TiO_2 from anatase to rutile structure at high temperatures [23,24].

3.1.3. UV–vis adsorption spectroscopic measurement and XPS analysis

Fig. 4 presents the UV–vis diffuse reflectance spectra of the ACFs supported TiO_2 photocatalysts calcined at 700 °C with different TiO_2 contents. The increase of absorbance in the UV region starts at around 400 nm for these three spectra. All of the spectra clearly show the characteristic absorption edge of anatase-form TiO_2 at about 380 nm. The adsorption edge without blue-shifting to a shorter wavelength region indicates small particle quantum size effect is not present for the produced photocatalysts. Carbon, with the color of black, exhibits strong adsorption in whole range of wavelength employed.

XPS analysis represents a valuable insight into the surface structure of ACFs supported TiO_2 photocatalyst. The photocatalyst employed with XPS analysis was calcined in a stream of Ar gas at 800 °C for 1.5 h. From the general XPS electron spectrum shown in Fig. 5a, the data imply that the photocatalyst surface contains only expected elements: titanium, oxygen, carbon, phosphorus and nitrogen, all of which come from the TiO_2 coating and carbon fibers surfaces. Spectra of individual lines of Ti2p, O1s and C1s measured at high resolution are shown in Fig. 5b–d. As shown in Fig. 5b, binding energies of $Ti2p_{1/2}$ and $Ti2p_{3/2}$ are 464.3 and 458.6 eV, respectively, which can been assigned to the $Ti^{4+}(TiO_2)$with a peak separation of 5.7 eV between those two peaks [25,26]. The obtained O1s spectrum shown in Fig. 5c has following three chemical states of oxygen corresponding to Ti–O bind of TiO_2 (B.E. = 529.7 eV), C–O bind of carbon fibers (B.E. = 532.7 eV) and hydroxyl groups (B.E. = 531.6 eV), which can be compared to the published data [26–28]. The hydroxyl groups on the surface of TiO_2 can be attributed to reaction of adsorbed H_2O with TiO_2 and formation of Ti–OH, such as $H_2O + Ti–O–Ti \rightarrow 2Ti–OH$ [3]. The surface hydroxyl groups, acting as an electron donor for photo-generated H^+, can be oxided into hydroxyl radicals($^{\bullet}OH$)which can attack almost all of organic pollutants [29]. The high resolution of C1s spectrum in Fig. 5d has been resolved into four individual component peaks representing graphitic carbon and CH_n (C–C and CH_n, B.E. = 284.6 eV) as the major peak, ether/hydroxyl groups (C–O, B.E. = 286.2 eV), carbonyl groups (C=O, B.E. = 287.1 eV) and also carboxyl groups (COOH, B.E. = 288.2 eV). The curve-fitting results of C1s spectrum are approximately in agreement with the previous data [30,31]. In addition, the asymmetric C1s spectrum with long tail and FWHM of the peak as 1.5 eV are also corresponding to a complete graphite lattice structure of ACFs [32]. Therefore, it suggests that the support, activated carbon fibers, has maintained its original surface properties and graphite lattice structure even after high temperature treatment.

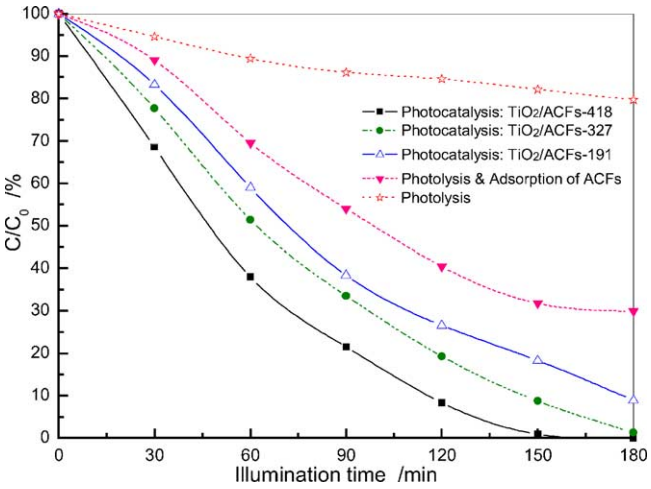

Fig. 6. Changes in relative concentration of MB with UV illumination time: comparison of photolysis, photolysis and adsorption of ACFs, and photocatalytic degradation by the TiO_2/ACFs.

Table 2
Comparison of MB removal rates at illumination time of 150 min

Type of operations	Photolysis	Photolysis and adsorption of ACFs	Photocatalysis		
			TiO_2/ACF-191	TiO_2/ACF-327	TiO_2/ACF-418
Removal rates (%)	17.85	68.2	81.75	91.3	99.1

3.2. Photocatalytic degradation of methylene blue

To evaluate the actual photocatalytic activity of the ACFs supported TiO_2 photocatalysts calcined at 700° for 1.5 h, comparison of three MB removal processes, namely, photolysis, photolysis and adsorption of unmodified ACFs, and photocatalytic decomposition by the TiO_2/ACFs photocatalysts, was carried out, and the results are shown in Fig. 6 and listed in Table 2. It can be found that methylene blue, a widely used organic color in dyeing and textile industries, can be degraded at a certain degree under UV irradiation, as shown with the curve of photolysis. The curve of photolysis and adsorption of the unmodified ACFs exhibits that the unmodified ACFs show a saturated adsorptive capacity for MB although the adsorptive capacity is very large due to the high S_{BET} of the ACFs. As shown in Fig. 6 and Table 2, the removal rates of photocatalytic degradation of MB with the prepared photocatalysts are much higher than that of the photolysis and adsorption of the unmodified ACFs, although the S_{BET} of the photocatalysts are much smaller than that of the ACFs. Obviously, photodecomposition of adsorbed MB enhances the adsorption rate of MB by keeping the adsorptive capacity of the support unsaturated. From other side of view, continued adsorption of MB by reborn carbon surfaces has provided the substrate for the photocatalysis of TiO_2 layer. These two mutually enhanced processes shown in Fig. 7, adsorption of the ACFs and photocatalysis of the deposited TiO_2, have been combined as the novel properties of the TiO_2/ACFs photocatalyst. In addition, the photodegradation rates of MB shown in Fig. 6 are increased with the increasing amount of loaded TiO_2. In fact, an optimized TiO_2 coating amount should exist to lead to the highest photocatalytic efficiency because TiO_2 coating amount and the S_{BET} for the TiO_2/ACFs photocatalyst are two mutually constrained factors in increasing photocatalytic efficiency although enhancing either of them will benefit to improving the photocatalytic efficiency. Three curves of the photocatalysis are consistent to this analysis.

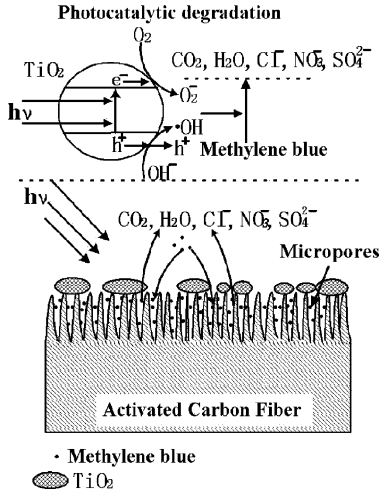

Fig. 7. Schematic diagram for the adsorption and photocatalytic degradation of MB on the TiO_2/ACFs.

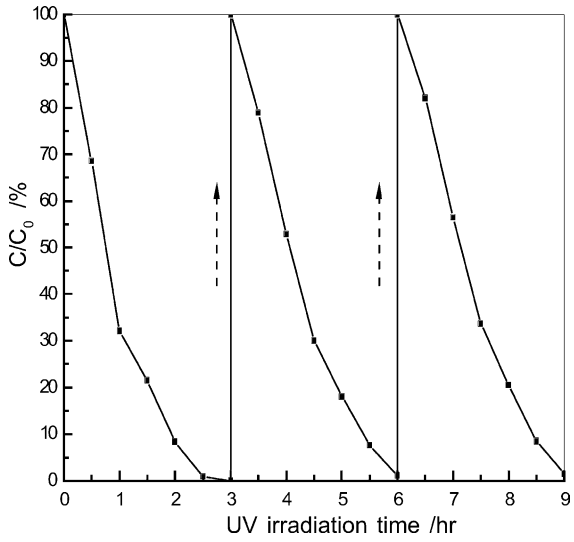

Fig. 8. Change in relative concentration of MB with cycling operations of photodegradation.

Therefore, for the TiO_2/ACFs photocatalysts employed, increasing TiO_2 coating amount would make the photodegradation rate higher although the S_{BET} of the photocatalyst will be lower.

To confirm cyclic usage is possible for produced ACFs supported TiO_2 photocatalysts, the photocatalyst TiO_2/ACFs-418 was selected. The change in relative concentration of MB with cycling operation is shown in Fig. 8. The photocatalytic reactivity of the present photocatalyst is just slightly reduced in stirred aqueous solution, indicating that cyclic usage of the photocatalyst is possible and its stability in treating polluted water is satisfactory. At the same time, it also proves that the final removal of MB from solutions is caused by the photocatalytic degradation other than the adsorption process that will lead to saturated adsorption of MB on the photocatalyst.

4. Conclusions

Our works described in this paper showed that activated carbon fibers supported TiO_2 photocatalyst could be prepared by means of the molecular adsorption–deposition method followed by calcination at high temperatures. The amount of deposited TiO_2 could be adjusted by controlling the $TiCl_4$ vapor pressure and adsorption time. Titanium dioxide was found to be loaded on almost all carbon fibers with a thickness of about 100 nm. The space between adjacent carbon fibers remained unfilled after coating of TiO_2 on ACFs, thus allowing UV light to penetrate into the felt-form photocatalyst to form a three-dimensional environment for photocatalytic degradation. In particular, the typical features of the photocatalyst prepared, felt-form and remaining space between carbon fibers, would make it very suitable for configurating an efficient photoreactor for purification of polluted water and air.

The unique anatase-form TiO_2 could be developed even as the calcination temperature rose up to 900 °C. Tight contact of thin TiO_2 film to carbon fibers was supposed to suppress the phase transformation of TiO_2 from anatase to rutile form, and to keep high crystallinity of anatase. The deposition of TiO_2 on carbon fibers and calcination at high temperatures had not damaged the micrographic structure and surface properties of ACFs, which would be advantageous for ACFs to keep its high adsorption capacity.

The developed photocatalyst exhibited high photocatalytic reactivity in photodegradation of highly concentrated mythylene blue solutions. The comparative experiments indicated that the photocatalyst produced had a combined effect of photocatalytic reactivity of anatase-type TiO_2 with adsorptive property of activated carbon fibers. Additionally, the cyclic usage is possible for the prepared photocatalyst as confirmed by photodegradation of methylene blue solutions.

References

[1] D.F. Ollis, H. Al-Ekabi (Eds.), Photocatalytic Purification and Treatment of Water and Air, Elsevier, Amsterdam, 1993.
[2] N. Serpone, E. Pelizzetti, Photocatalysis: Fundamentals Applications, Wiley, New York, 1989.
[3] M.R. Hoffmann, S.T. Martin, W. Choi, D.W. Bahnemann, Chem. Rev. 95 (1995) 69.
[4] H. Hidaka, J. Zhao, E. Pelizzetti, N. Serpone, J. Phys. Chem. 96 (1992) 2226.
[5] A.K. Ray, Chem. Eng. Sci. 54 (1999) 3113.
[6] H. Yamashita, M. Harada, A. Tanii, M. Honda, M. Takeuchi, Y. Ichihashi, M. Anpo, N. Iwanoto, N. Itoh, T. Hirao, Catal. Today 63 (2000) 63.
[7] H. Hidaka, Y. Asai, J. Zhao, K. Nohara, N. Serpone, E. Pelizzetti, J. Phys. Chem. 99 (1995) 8244.
[8] D.H. Kim, M.A. Anderson, Environ. Sci. Technol. 28 (1994) 497.
[9] T. Torimoto, Y. Okawa, N. Takeda, H. Yoneyama, J. Photochem. Photobio. A: Chem. 103 (1997) 153.
[10] C.H. Ao, S.C. Lee, J. Photochem. Photobio. A: Chem. 161 (2004) 131.
[11] H. Yoneyama, T. Torimoto, Catal. Today 58 (2000) 133.
[12] S. Nagaoka, Y. Hamasaki, S. Ishihara, M. Nagata, K. Iio, C. Nagasawa, H. Ihara, J. Mol. Catal. A: Chem. 177 (2002) 255.
[13] J.J. Freeman, F.G.R. Gimblett, R.A. Roberts, K.S.W. Sing, Carbon 25 (1987) 559.
[14] K. Kaneko, Y. Nakahigashi, K. Nagata, Carbon 26 (1988) 327.
[15] G.G. Jayson, T.A. Lawless, D. Fairhust, J. Colloid Interf. Sci. 86 (1982) 397.
[16] M. Anpo, Y. Ichihashi, M. Takeuchi, H. Yamashita, Res. Chem. Intermed. 24 (1998) 151.
[17] M. Nozawa, K. Tanigawa, M. Hosomi, T. Chikusa, E. Kawada, Water Sci. Technol. 44 (2001) 127.
[18] A. Matsumoto, K. Tsutsumi, K. Kaneko, Langmiur 8 (1992) 2515.
[19] T. Torimto, S. Ito, S. Kuwatata, H. Yoneyama, Environ. Sci. Technol. 30 (1996) 1275.
[20] Z. Ding, X.J. Hu, G.Q. Lu, P. Yue, P.F. Greenfield, Langmiur 16 (2000) 6216.
[21] D. Takenori, I. Kiyohisa, J. Electrochem. Soc. 147 (2000) 2263.
[22] J. Sabate, M.A. Anderson, H. Kikkawa, S. Cervera-March, C.G. Hill Jr., J. Catal. 134 (1992) 36.
[23] T. Tsumura, N. Kojitani, H. Umemura, M. Toyoda, M. Inagaki, Appl. Surf. Sci. 196 (2002) 429.
[24] T. Tsumura, N. Kojitani, I. Izumi, N. Iwashita, M. Toyoda, M. Inagaki, J. Mater. Chem. 12 (2002) 1391.
[25] C. Wagner, G. Muilenbergy (Eds.), Handbook of X-ray Photoelectron Spectroscopy, Perkin-Elmer Corporation, Minnesota, 1979, p. 38.
[26] F.M. Liu, T.M. Wang, Appl. Surf. Sci. 195 (2002) 284.
[27] S. Biniak, G. Szymanski, J. Siedlewski, A. Swiatkowski, Carbon 35 (1997) 1799.
[28] J.G. Yu, X.J. Zhao, Q.N. Zhou, Thin Solid Films 379 (2000) 7.
[29] A. Fujishima, T.N. rao, D.A. Tryk, J. Photochem. Photobio. C: Photochem. Rev. 1 (2000) 1.
[30] T. Takahagi, A. Ishitani, Carbon 22 (1984) 43.
[31] M.C. Paiva, C.A. Bernardo, M. Nardin, Carbon 38 (2000) 1323.
[32] T. Takahagi, A. Ishitani, Carbon 26 (1988) 389.
[33] M.A. Short, P.L. Walker, Carbon 1 (1963) 3.